

11

Pharmacodynamics and Pharmacokinetic/ Pharmacodynamic Relationships

Pharmacodynamics is the study that establishes and elucidates relationships between concentrations of a drug at the receptor or target organ (effect site) and the intensity of its pharmacological effect. Pharmacodynamic studies can provide a means for identifying important pharmacological and toxicological properties of a drug in animals and humans, including, e.g., efficacious target concentrations, drug safety margin, potential risk factors, and the presence of active metabolites (Holford and Sheiner, 1982). In many cases, it is difficult to measure drug concentrations right at the effect site, and thus therapeutic drug monitoring is often performed by measuring drug concentrations in plasma or other readily accessible body fluids, which may not be directly related to the intensity of the drug effect. Pharmacokinetic and pharmacodynamic modeling contributes to a better understanding of the relationship between drug concentrations in biological fluids, where concentrations are measured, and those in the effect site. In this chapter, pharmacodynamics and various pharmacokinetic/pharmacodynamic models and physiological and experimental factors that may complicate pharmacodynamic studies are discussed.

11.1. PHARMACODYNAMICS

11.1.1. Definition

Pharmacodynamics deals with the relationship between drug concentrations at the effect site or concentrations (usually unbound concentrations) in plasma in equilibrium with effect site concentrations, and the magnitude of the observed pharmacological effect of the drug.

11.1.2. Effect Site

The effect site (site of action) of a drug can be a target receptor/enzyme(s) or an organ(s) where the initial pharmacological responses to the drug are produced.

For instance, the effect site of antidepressant agents would be the brain, and thus drug concentrations in the cerebrospinal fluid might be more relevant in establishing pharmacodynamic relationships than the plasma or blood drug concentrations under nonsteady state conditions. This is because drug concentrations between the brain and the blood can differ significantly at nonsteady state owing to delay in drug transport across the blood–brain barrier. On the other hand, the blood can be considered an effect site for certain antibiotics that target blood pathogens. In many cases, the experimentally measured pharmacological effects of a drug *in vivo* are only remotely or indirectly related to the initial stimulus it produces at the effect site, because there is often a series of biological events after the initial stimulus that lead to the observed effects.

Drug concentration at the effect site: The most direct link between concentration and effect can be made by simultaneous measurements of drug concentrations at the effect site and the corresponding pharmacological effects. However, owing to experimental difficulties in simultaneous measurements, the pharmacodynamic relationship is sometimes investigated when drug concentrations at the effect site are considered to be in equilibrium with those in readily available biological fluids such as plasma or blood after steady state infusion or multiple dosing.

11.1.3. Pharmacological Effects

The pharmacological activity of a drug generally includes a series of sequential events, i.e., interaction of drug molecules with their action sites or receptors, induction of a stimulus to the effector systems, and subsequent production of the effect (observed pharmacological endpoints). For instance, although warfarin rapidly blocks the synthesis of the prothrombin complex activity P, it takes several days before the levels of circulating P are reduced sufficiently to decrease normal prothrombin activity, a pharmacological endpoint. Therefore, the intensity of the pharmacological response observed does not necessarily reflect the result of direct interaction of drug molecules with target receptors or enzymes, especially when the receptors and the effector systems are not located in the same organs or tissues.

11.1.3.1. Characteristics of Pharmacological Responses

The reliable and reproducible measurement of drug's pharmacological effects is probably the most important factor required to establish meaningful pharmacodynamic relationships. There are several criteria by which to define the various characteristics of pharmacological responses.

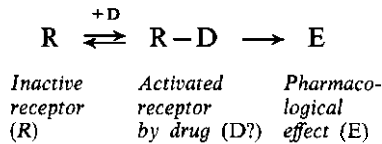
(a) *All-or-None vs. Graded Responses.* The fixed (all-or-none) response of a drug implies that there is or is not a response, e.g., mortality rate, whereas the graded response may vary with dose or drug concentration. The graded response can be further divided into absolute and relative responses, which can be measured in a definitive or relative manner, respectively. For instance, blood pressure or body temperature can be viewed as an absolute response, while percent muscle contractility is considered a relative response.

(b) *Direct vs. Indirect Responses.* For some drugs, the pharmacological endpoints may directly reflect the capacity (intrinsic activity) and affinity (potency) of the interaction between a drug and specific receptors/enzymes. In some cases, however, the pharmacological response to a drug may not be directly related to its binding rate to receptors, but result from serial biological events after its initial interaction with receptors. For instance, the gradual decrease in blood pressure brought about by a diuretic can be viewed as an indirect response.

(c) *Reversible vs. Irreversible Responses.* A reversible response means that the baseline effect prior to treatment can be restored when the drug is no longer being administered. On the other hand, an irreversible response implies that the drug causes changes in certain *in vivo* physiological or biological conditions such that the baseline effect cannot be restored when the drug is withdrawn. For most drugs, the effect is reversible. The pharmacological effect of drugs such as antibiotics or antineoplastic agents can be viewed as irreversible.

11.1.3.2. Receptor Theory

The pharmacological effect of a drug is mediated by the initial interaction of the drug molecules with particular receptor(s) according to the following scheme:



11.1.4. Differences among Pharmacokinetics, the Pharmacokinetic/Pharmacodynamic Relationship, and Pharmacodynamics

When dealing with the overall time course of a dose–effect relationship, there are three different stages to be considered, as indicated in Fig. 11.1 (Holford and Sheiner, 1981).

STAGE 1: The relationship between the dose and the time course of drug concentrations in biological fluids (*pharmacokinetics*).

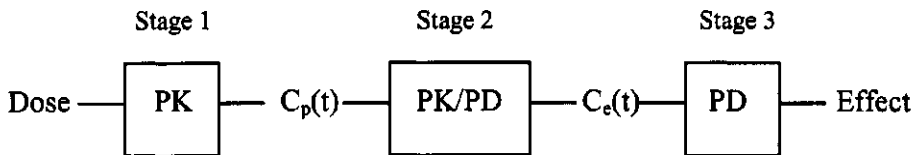


Figure 11.1. Overall relationships between the administered dose and the intensity of the measured pharmacological effects at the three different stages $C_e(t)$: concentration of drug at the effect site at time t , $C_p(t)$: concentration of drug in biological fluids such as plasma or blood at time t , PD: pharmacodynamics, PK: pharmacokinetics, PK/PD: pharmacokinetic/pharmacodynamic relationship.

STAGE 2: The time-dependent relationship between the drug concentrations in biological fluids such as plasma and at the effect site, which can be established by linking pharmacokinetics and pharmacodynamics of the drug with PK/PD modeling approaches (*pharmacokinetic and pharmacodynamic relationship*).

STAGE 3: The relationship between drug concentration at effect site and the observed pharmacological effects (*pharmacodynamics*).

The direct pharmacodynamic (PD) relationship can be established between plasma (or blood) concentrations and the observed pharmacological effects of a drug without pharmacokinetic/pharmacodynamic (PK/PD) modeling when: (1) drug concentrations at the effect site have reached equilibrium with concentrations in the plasma, especially free drug concentrations, after steady state infusion or multiple doses; or (2) the plasma (or blood) pool is the drug action site such as is the case with antibiotics. Except for these two cases, PK/PD relationships of a drug may have to be examined to establish its true PD profiles. PK/PD modeling can offer:

1. A better understanding of pharmacological behaviors of a drug (duration of action, delayed effect, circadian rhythm, biofeedback, etc).
2. Opportunity for recognizing the presence of active (or inhibitory) metabolite(s).
3. A better strategy for a therapeutic dose regimen.
4. A better understanding of potential drug–drug interactions.

11.1.5. Important Factors in Pharmacodynamic Study Designs

A thorough understanding of PK profiles is a prerequisite for elucidating reliable PD profiles. Factors in three different areas, i.e., animals, materials, and researchers, that have to be considered for reliable PK and PD experiments are noted below (Levy, 1985).

11.1.5.1. Animals

- Maintain the same strain and age from the same supply source.
- Use at least three animals/sex for study.
- If needed, carry out the same treatment on control groups, such as administration of dosing vehicle with no drug or sham operation.
- Preferentially, perform the studies at the same time of day to reduce any variability due to the circadian rhythm in animal physiology.
- Preferentially, avoid coprophagy when studies are performed in rodents.
- Do not draw too much body fluid from animals for sampling, especially in small animals. In general, less than 10% of the total blood volume can be drawn from small animals in a week.

11.1.5.2. Materials

- Identify polymorphism of crystallinity of the drug dosed, especially for suspension formulation for oral dosing. In general, an amorphous drug shows an apparently

higher aqueous solubility, which can lead to faster and more extensive oral absorption compared to the more stable crystalline forms.

- Maintain homogeneity of dosing formulations, especially when precipitation of the drug in the GI tract or injection site is expected.
- Use an optimal dosing volume (e.g., <5 or <10 ml/kg of oral dosing volume in rats when fed or fasted, respectively, to avoid potential overflow of dosing solution from the stomach to the lungs).

11.1.5.3. Researcher

- Determine the pharmacological response in *in vivo* experiments by the same researcher, especially when subjective quantification methods of drug effects are used.

11.1.6. Effects of Protein Binding on Pharmacodynamics

It has been suggested that the *in vivo* pharmacological efficacy of a drug is mediated solely by the unbound drug in plasma, because only unbound drug molecules from plasma proteins are available for interaction with target receptors. The extent of protein binding is especially important in assessing the pharmacodynamics of drugs in disease states, in which the amount of plasma protein content may be altered. For instance, epilepsy in individuals with renal failure receiving phenytoin is adequately controlled at a lower total concentration of the drug as compared to those with normal renal function, because the unbound drug concentrations are the same between the two groups owing to reduced protein binding in patients with renal failure (du Souich *et al.*, 1993).

11.2. PHARMACODYNAMIC MODELS

11.2.1. Definition

Pharmacodynamic models are mathematical schemes based on classical receptor theory for an empirical description of the intensity of a pharmacological response to a drug as a function of its concentrations at *the effect site*.

11.2.2. Implications of Pharmacodynamic Models

Pharmacodynamic models are useful for describing the apparent pharmacodynamic profiles of a drug and also for gaining some insight into its underlying physiological or biological processes (Holford and Sheiner, 1982; Ritschel and Hussain, 1984; Schwinghammer and Kroboth, 1988). Several pharmacodynamic models have been developed based on two assumptions: (a) drug response is reversible and, (b) there is only one type of receptor with one binding site for a drug.

11.2.3. Types of Pharmacodynamic Models

11.2.3.1. Linear Model

The linear pharmacodynamic model is useful when the efficacy of a drug is proportional to its concentrations at the effect site. The linear model can be derived from the E_{\max} model, when its concentrations at the effect site is significantly lower than EC_{50} (see the E_{\max} model).

$$(11.1) \quad E = S \cdot C_e + E_0$$

C_e is the drug concentration at the effect site, E is the intensity of the effect, E_0 is the baseline effect in the absence of the drug, and S is the slope.

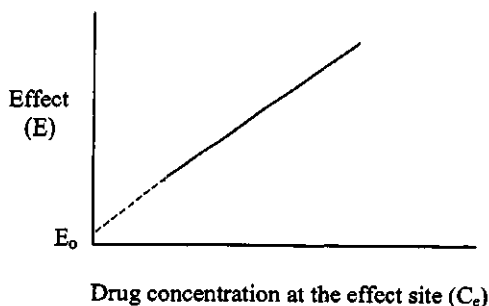


Figure 11.2. Linear model.

11.2.3.2. Log-Linear Model

The log-linear model is based on the empirical observation that a plot of effect vs. log concentration of many drugs exhibits a linear approximation between 20 and 80% of the maximum effect. Like the linear model, the concentration-effect relationship within this range can be analyzed using linear regression:

$$(11.2) \quad E = S \cdot \log C_e + I$$

S is the slope and I is an empirical constant with no physiological meaning.

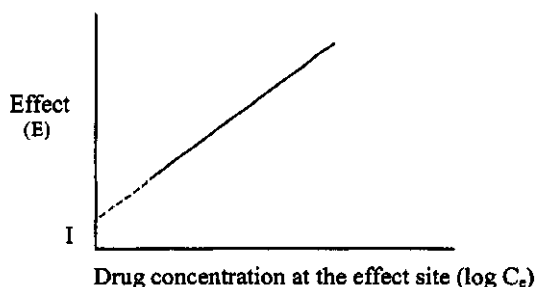


Figure 11.3. Log-linear model.

11.2.3.3. E_{\max} Model

The E_{\max} model can describe the concentration–effect curve over the full range from the baseline effect to the maximum effect of a drug. Accurate measurement of both E_{\max} and EC_{50} are critical in the E_{\max} model. In fact, only a few drugs have been shown to have this relationship *in vivo* mainly owing to the difficulties involved in conducting studies over a wide range of concentrations, especially at high concentrations because of the concomitant potential toxicity:

$$(11.3) \quad E = \frac{E_{\max} \cdot C_e}{EC_{50} + C_e} (+ E_0)$$

where E_{\max} the maximum effect, EC_{50} is the drug concentration that produces 50% of the maximum effect, and E_0 is the baseline effect in the absence of any drug.

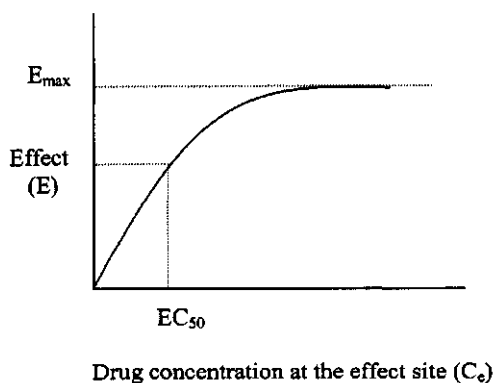


Figure 11.4. E_{\max} model.

11.2.3.4. Sigmoid E_{\max} Model

The sigmoid E_{\max} model can be used when the concentration–effect curve exhibits more an S-shape pattern than a simple hyperbola (the E_{\max} model), and is steeper or shallower than predicted by the E_{\max} model. The sigmoid function originally proposed by Hill (1910) is often called the Hill equation:

$$(11.4) \quad E = \frac{E_{\max} \cdot C_e^n}{EC_{50}^n + C_e^n} (+ E_0)$$

where n is the Hill coefficient that affects the slope of the curve: at $n > 1$ the curve becomes sigmoid with a steeper slope than the E_{\max} model at concentrations around EC_{50} ; at $n = 1$: the curve is identical to the usual hyperbola of the E_{\max} model; and at $n < 1$ the curve is steeper at low concentrations, but shallower at high concentrations than the E_{\max} model.

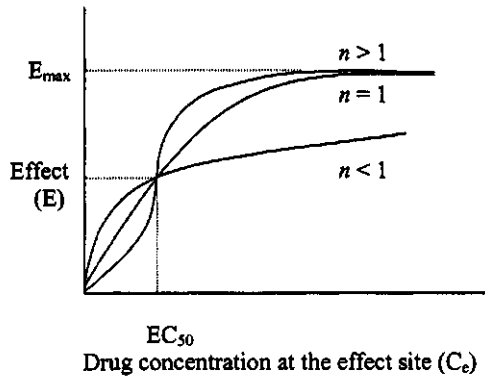


Figure 11.5. Sigmoid E_{max} model.

11.2.3.5. Inhibitory E_{max} Model

The same pharmacodynamic models discussed earlier can be used to describe the inhibitory effect of a drug by arranging the equations so that the observed effect becomes the difference between the drug's baseline effect (E_0) and inhibitory effect. For instance, the E_{max} model can be adapted to express the inhibitory response of a drug with maximum inhibitory effect (I_{max}) and IC_{50} , at which 50% of I_{max} is produced. This model is useful for investigating the inhibitory effects of a drug without transforming the data:

$$(11.5) \quad E = E_0 - \frac{I_{max} \cdot C_e}{IC_{50} + C_e}$$

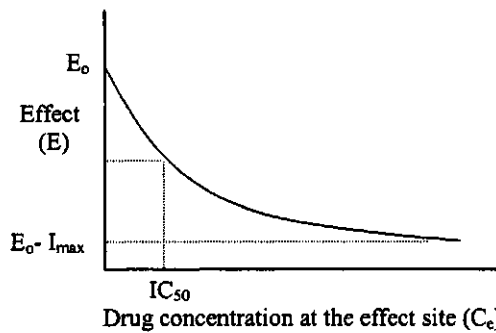


Figure 11.6. Inhibitory E_{max} model.

11.2.3.6. Models for Multiple Receptors

Only pharmacodynamic models applicable for drugs binding to a single type of receptor with one binding site have been described so far. For an increasing number of drugs, however, it is becoming evident that there may be either multiple receptors

Table 11.1. A Summary of Various Pharmacodynamic Models

Model	E	Characteristics
Linear	$S \cdot C_e + E_0$	Predicts the baseline effect when the concentration is zero Unable to define the maximum effect at high concentrations Error-prone at high or low drug concentrations
Log-linear	$S \cdot \log C_e + I$	Suitable for predicting drug effects over 20–80% of the maximum effect Unable to define the baseline and the maximum effects
E_{max}	$\frac{E_{max} \cdot C_e}{EC_{50} + C_e} + E_0$	Able to describe the pharmacodynamic relationship over a wide range of drug concentrations Predicts the baseline and the maximum effects
Sigmoid E_{max}	$\frac{E_{max} \cdot C_e^n}{EC_{50}^n + C_e^n} + E_0$	Able to describe an S-shape pattern of effect curve by adjusting n values Predicts the baseline and the maximum effects

and/or multiple binding sites with different activities (Campbell, 1990; Paalzow *et al.*, 1985). These can cause cascade- or U-shape concentration–effect curves. For instance, the analgesic effect of clonidine is mediated by two agonistic effects, both of which can be described by different E_{max} models, producing a stepwise increase in effect with concentration [Eq. (11.6), Fig. 11.7A]. On the other hand, for blood pressure, clonidine exhibits a hypotensive activity at low concentrations, but a hypertensive activity at higher concentrations owing to concentration-dependent binding to presynaptic α_2 and postsynaptic α_1 receptors, respectively, producing a U-shape concentration–effect curve [Eq. (11.7), Fig. 11.7B].

DUAL AGONISTIC RECEPTORS (cascade shape concentration-effect curve, Fig. 11.7A):

$$(11.6) \quad E = \underbrace{\frac{E_{max,1} \cdot C_e^n}{EC_{50,1}^n + C_e^n}}_{E_1} + \underbrace{\frac{E_{max,2} \cdot C_e^m}{EC_{50,2}^m + C_e^m}}_{E_2}$$

BIPHASIC RECEPTORS (agonist–antagonist, U- or bell-shape concentration–effect curve, Fig. 11.7B):

$$(11.7) \quad E = \underbrace{\frac{E_{max,1} \cdot C_e^n}{EC_{50,1}^n + C_e^n}}_{E_1} - \underbrace{\frac{E_{max,2} \cdot C_e^m}{EC_{50,2}^m + C_e^m}}_{E_2}$$

where $E_{max,1}$ and $E_{max,2}$ are, respectively, the maximum effect for each of two different receptors, $EC_{50,1}$ and $EC_{50,2}$ are the drug concentrations that produce 50% of $E_{max,1}$ or $E_{max,2}$, and n and m are the Hill coefficients.

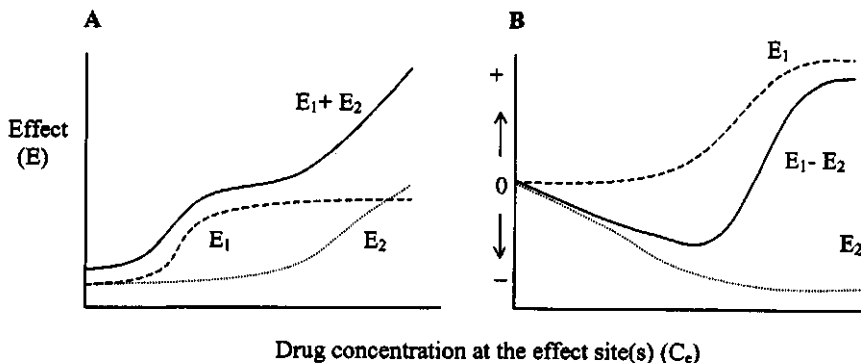


Figure 11.7. Drug concentration at the effect site(s) vs. effect for dual agonistic receptors (A) and agonistic-antagonistic receptors (B).

11.2.4. Model Selection

The initial decision to select one particular pharmacodynamic model(s) over another for a certain data set should be based on: (a) the need for estimating particular parameters (EC_{50} , E_{max} , E_0 , etc), and (b) the ability of the model and availability of data suitable to provide estimates of those parameters. When more than one model is chosen and there are no obvious deficiencies in the models for parameter estimation, the choice of a model can be made according to certain statistical indications (Schwinghammer, 1988) including: (a) the smaller sum of squares of residuals (the differences between the observed and predicted effect values), (b) the smaller asymptotic standard deviations, (c) the smaller 95% confidence interval, (d) the smaller Akaike's Information Criterion (AIC) value, and the greater r^2 values (see Chapter 2).

11.2.5. Difficulties in Pharmacodynamic Modeling

In many cases, it is difficult to measure drug concentrations at the effect site because of limited sample availability or inaccessibility of the effect site, or to quantitatively assess the pharmacological effect owing to the complicated mechanisms and physiological variations involved (Levy, 1985; Oosterhuis and van Boxtel, 1988; Schwinghammer and Kroboth, 1988). In addition, there are numerous endogenous and exogenous factors that may have confounding effects on the study of pharmacodynamics of a drug in *in vivo* systems as summarized in the following:

- Lack of correlation between the plasma drug concentrations and concentrations at the effect site.
- Difficulties in reliable and reproducible measurements of pharmacological effects.
- Difficulties in quantifying direct pharmacological effects of a drug.

- Complicated pharmacological effects: (a) multiple receptors or target tissues; (b) concentration-dependence in effect (e.g., agonist at low concentrations, but antagonistic at high concentrations).
- The presence of endogenous agonists or antagonists at variable concentrations.
- Difficulties in distinguishing pharmacodynamic variability from pharmacokinetic variability: Pharmacokinetic issues such as active (or inhibitory) drug metabolites can complicate the isolation of pharmacological effects related solely to the parent drug.
- Development of tolerance or sensitization after the prolonged exposure of a drug: (a) tolerance (down-regulation), i.e., decrease in the density of receptors related to a drug after long-term administration (tachyphylaxis); (b) sensitization (up-regulation), i.e., increase in the density of receptors causing an overshoot effect after withdrawal of a drug.
- Physiological homeostatic responses (biofeedback mechanisms): administration of a drug can influence the concentration of endogenous agonists acting on the same receptor.
- Disease states: disease-induced pharmacodynamic alterations may not necessarily be the result of changes in receptor characteristics or effector mechanisms.
- Interindividual or intraindividual variability in pharmacodynamics owing to genetic or environmental factors.
- Stereoisomerism: drug concentration–effect relationships can be further complicated when the drug is a mixture of racemates or diastereomers and its isomers have different activities, e.g., labetalol and propranolol. If a stereospecific assay for a drug is not available or there is interconversion among isomers with different activities, establishing a meaningful relationship between drug concentration and effect becomes especially difficult.
- Drug–drug interaction in pharmacodynamics by the coadministered drug.

11.3. PHARMACOKINETIC/PHARMACODYNAMIC MODELING

11.3.1. Definition

Pharmacokinetic/pharmacodynamic (PK/PD) mathematical modeling to elucidate the relationship between drug concentrations in plasma and at the effect site by examining the plasma drug concentration *vs.* effect relationship, thus revealing the true pharmacodynamic profiles of a drug, i.e., the relationship between drug concentrations at the effect site and its pharmacological effects.

11.3.2. Implications of Pharmacokinetic/Pharmacodynamic Modeling

Simultaneous measurement of drug concentrations at the effect site $[C_e(t)]$ and its pharmacological effect $[E(t)]$ is the most desirable approach to reveal the true pharmacodynamic (PD) profiles of a drug. It is, however, seldom feasible to measure $C_e(t)$. In many *in vivo* studies, PD analyses are frequently performed based on drug concentrations in plasma $[C_p(t)]$, assuming that $C_p(t)$ is in rapid equilibrium with $C_e(t)$, and that unbound drug concentrations are the same in both the plasma and

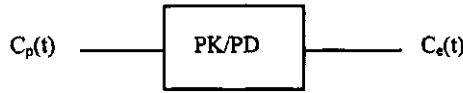


Figure 11.8. Pharmacokinetic/pharmacodynamic modeling to elucidate the relationship between drug concentrations in plasma [$C_p(t)$] and at the effect site [$C_e(t)$] under nonsteady state conditions.

at the effect site. If $C_p(t)$ is not in rapid equilibrium with $C_e(t)$, i.e., there is a delay in drug distribution from the plasma to the effect site or vice versa, or the system is subject to time-dependent kinetic and/or dynamic changes, the pharmacological response will take time to develop, and there will be no apparent relationship between $C_p(t)$ and $E(t)$. PK/PD modeling can elucidate the relationship between $C_p(t)$ and $C_e(t)$ by integrating available information on $C_p(t)$ vs. $E(t)$, and reveal the true PD of a drug between $C_e(t)$ and $E(t)$ without establishing equilibrium between $C_p(t)$ and $C_e(t)$ (Fig. 11.8). A schematic description of PK/PD model developing processes when there is a time-delay discrepancy in the relationship between plasma drug concentrations and observed pharmacological effects under nonsteady state conditions is shown in Fig. 11.9.

11.3.3. Types of Pharmacokinetic/Pharmacodynamic Models

11.3.3.1. Effect Compartment (or Link) Model

The effect compartment model assumes that the differences between $C_p(t)$ and $C_e(t)$ are due to a delay in drug distribution from the plasma (the central compartment) to the effect site (the effect site compartment). The model is designed to eliminate the time-related discrepancy between $C_p(t)$ and E at different time points

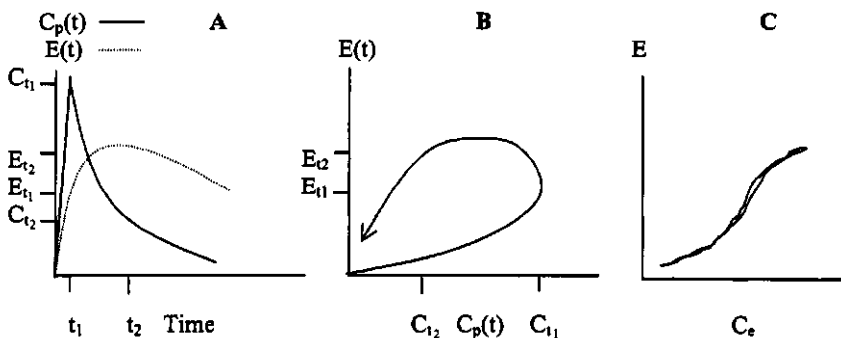


Figure 11.9. Schematic representations of pharmacokinetic/pharmacodynamic (PK/PD) modeling processes: (A) Plasma drug concentration–time and effect–time profiles after a short intravenous infusion up to time t_1 . (B) Plasma drug concentration–effect plot showing an apparent discrepancy between the plasma drug concentration levels (C_{p1} and C_{p2}) and the intensity of the effect at different time points (t_1 and t_2) (see Counterclockwise hysteresis). (C) The PK/PD model predicts $C_e(t)$ based on $C_p(t)$, and reveals the true PD relationships between C_e and E by eliminating the time delay between $C_p(t)$ and $E(t)$. $C_p(t)$ and C_e : drug concentration in plasma at time t and at the effect site, respectively, and E : the intensity of effect.

caused by *distributional delay*, by introducing the so-called equilibration rate constant, k_{eo} (Holford and Sheiner, 1981). Figure 11.10 is a schematic representation of the effect compartment model connected to the central compartment of a multicompartment model system after intravenous bolus injection of a drug into the central compartment.

The following steps are taken for the effect compartment model approaches:

STEP 1: Derive an equation describing $C_e(t)$ from $C_p(t)$ based on a PK model for $C_p(t)$ and k_{eo} . For instance, when the plasma drug exposure is adequately described with a single-compartment model and the drug is given intravenously, $C_e(t)$ can be expressed as a function of $C_p(t)$ and microconstants, k_{el} and k_{eo} :

$$(11.8) \quad C_e(t) = \frac{D \cdot k_{eo}}{V \cdot (k_{eo} - k_{el})} \cdot (e^{-k_{el} \cdot t} - e^{-k_{eo} \cdot t})$$

and

$$(11.9) \quad C_p(t) = \frac{D}{V} \cdot e^{-k_{el} \cdot t}$$

where V is volume of distribution of the drug.

STEP 2: Select a proper PD model and incorporate $C_e(t)$ obtained from step 1 into it. For instance, if an E_{max} model is chosen, $E(t)$ can be written as a function of $C_e(t)$:

$$(11.10) \quad E(t) = \frac{E_{max} \cdot C_e(t)}{EC_{50} + C_e(t)}$$

Equations (11.8)–(11.10) can be simultaneously fitted to experimental data on $C_p(t)$ and $E(t)$ to estimate k_{eo} , E_{max} , and EC_{50} , using an appropriate nonlinear regression method.

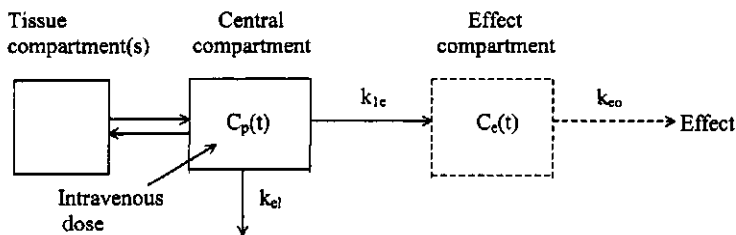


Figure 11.10. Schematic description of the effect compartment model. The hypothetical effect compartment is connected to the central compartment, usually, a plasma pool. When more than one compartment is required for describing the pharmacokinetics of a drug, the tissue compartments can be connected to the central one. Drug concentration at the effect site is governed by drug concentrations in the central compartment, and the extent of k_{eo} . $C_p(t)$ and $C_e(t)$: drug concentrations in plasma and at the effect site, respectively; $E(t)$: effect; k_{1e} , k_{el} , and k_{eo} : distribution rate constant from the central to the effect compartment, elimination rate constant from the central compartment, and equilibration rate constant, respectively.

11.3.3.2. Indirect Response Model

The premise of the indirect response model is that a slow onset of drug response or a slow return to baseline, i.e., time-related discrepancies in the $C_p(t)$ – E relationship, can be due to indirect responses to the drug stemming from drug-related stimulation or inhibition, respectively, of the factors controlling either the production or the loss of the effect (Fig. 11.11) (Bellissant *et al.*, 1998; Dayneka *et al.*, 1993).

The rate of change of the effect in the absence of the drug can be described by

$$(11.11) \quad \frac{dE(t)}{dt} = k_{in} - k_{out} \cdot E(t)$$

where k_{in} and k_{out} , are, respectively, the zero-order and the first-order rate constant for production and loss of an effect. The following steps can be taken with the indirect response model.

STEP 1: Identify an equation for describing the rate of change of the effect (or response) over time in the presence of the drug. There are four different equations available, depending on whether the production or loss of response variables is stimulated or inhibited:

$$\begin{aligned} \frac{dE(t)}{dt} &= k_{in} \cdot S(t) - k_{out} \cdot E(t), \text{ when the drug stimulates the effect} \\ &= k_{in} \cdot I(t) - k_{out} \cdot E(t), \text{ when the drug inhibits the effect} \\ &= k_{in} - k_{out} \cdot S(t) \cdot E(t), \text{ when the drug stimulates loss of the effect} \\ &= k_{in} - k_{out} \cdot I(t) \cdot E(t), \text{ when the drug inhibits loss of the effect} \end{aligned}$$

The stimulation function $S(t)$, and the inhibition function $I(t)$, can be expressed as follows:

$$(11.12) \quad S(t) = 1 + \frac{E_{max} \cdot C_p(t)}{EC_{50} + C_p(t)}$$

$$(11.13) \quad I(t) = 1 - \frac{C_p(t)}{IC_{50} + C_p(t)}$$

where EC_{50} and IC_{50} are, respectively, the drug concentrations producing 50% of the maximum stimulation and 50% of maximum inhibition achieved at the effect site.

STEP 2: The equation chosen is fitted to the experimental data on $C_p(t)$ and $E(t)$ to estimate those parameters using an appropriate nonlinear regression method.

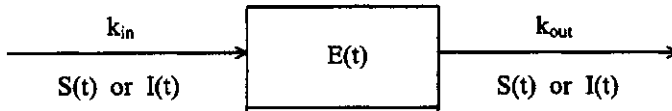


Figure 11.11. Schematic representation of the indirect response model. $E(t)$: Effect; $S(t)$ and $I(t)$: stimulation and inhibition functions, respectively; k_{in} and k_{out} : the zero-order rate constant for production and the first-order rate constant for loss of the effect, respectively.

11.4. PROTERESIS OR HYSTERESIS

When $C_p(t)$ after a single dose or multiple doses is plotted against the corresponding $E(t)$ and connected in a time sequence, the intensity of the effect is sometimes different at different time points even at the same concentrations (Campbell, 1990; Oosterhuis and van Boxtel, 1988), and it is the pattern of this relationship as a function of time that defines proteresis or hysteresis in pharmacodynamics.

Proteresis (Clockwise Hysteresis) and Hysteresis (Counterclockwise Hysteresis): If the intensity of the drug effect is higher at the earlier time points than at the later

Table 11.2. Factors Causing a Proteresis or Hysteresis Loop in a Plasma Drug Concentration $[C_p(t)]$ vs. Effect $[E(t)]$ Plot

Pattern of a $C_p(t)$ vs. $E(t)$ plot connected in time sequence	Factors causing the time-related discrepancies in the apparent concentration–effect relationship
<i>Proteresis</i>	<ul style="list-style-type: none"> Development of tolerance: a dampened response to the drug, after prolonged or repeated exposure (diazepam, morphine) Formation of antagonistic metabolites: antagonistic metabolites competing with the drug for the same binding sites on the receptor (pentobarbital) Down-regulation: decrease in the number of receptors after the prolonged exposure of the drug (isoproterenol) Biofeedback regulation (almitrine, nifedipine, tyramine)
<i>Hysteresis</i>	<ul style="list-style-type: none"> Distribution delay^a: the nonequilibrium condition of drug concentrations between the plasma and the effect site owing to slow drug distribution from the plasma, sampling site, to the effect site (9-tetrahydrocannabinol, thiopental) Response delay: the delayed pharmacological response resulting from a series of biological events upon the initial stimulus by the drug interacting with a specific receptor at the effect site (corticosteroids, warfarin) Sensitization of receptors (angiotensin, propranolol) Formation of agonistic (active) metabolites (fenfluramine, camazepam, midazolam) Up-regulation: increase in the number of receptors after the prolonged exposure of the drug (propranolol)

^aThe most common cause for the hysteresis.

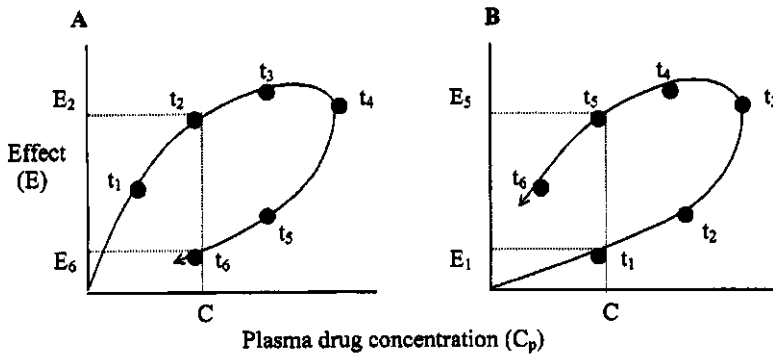


Figure 11.12. Proteresis (A) and hysteresis (B) relationships between plasma drug concentrations (\bullet) from time t_1 to t_6 and the corresponding effect levels of a drug. A: The effect (E_2) at the earlier time point (t_2) is more pronounced than that (E_6) at the later time point (t_6) despite the same plasma concentration (C). B: The effect (E_1) at t_1 is lower than that (E_5) at t_5 at the same concentration (C).

ones at the same plasma drug concentrations, the clockwise pattern of the loop connecting concentration vs. effect data points in a time sequence reflects proteresis (or clockwise hysteresis) (Fig. 11.12A).

If the intensity of the drug effect is higher at the later time points than at the earlier ones at the same plasma drug concentrations, this counterclockwise pattern of the loop connecting data points in a time sequence or an apparent delay in effect is referred to as (counterclockwise) hysteresis (Fig. 11.12B).

In both proteresis and hysteresis, the pharmacological response is considered to be direct and reversible. These time-related discrepancies in the apparent concentration–effect relationship revealed by proteresis or hysteresis loops can be due to a lack of equilibrium in drug concentrations between the plasma and the effect site, but also can be due to many other factors (Table 11.2).

REFERENCES

- Bellissant E. *et al.*, Methodological issues in pharmacokinetic-pharmacodynamic modelling, *Clin. Pharmacokinet.* **35**: 151–166, 1998.
- Campbell D. B., The use of kinetic-dynamic interactions in the evaluation of drugs, *Psychopharmacology* **100**: 433–450, 1990.
- Dayneka N. L. *et al.*, Comparison of four basic models of indirect pharmacodynamic responses, *J. Pharmacokinet. Biopharm.* **21**: 457–478, 1993.
- du Souich T. *et al.*, Plasma protein binding and pharmacological response, *Clin. Pharmacokinet.* **24**: 435–440, 1993.
- Hill. A. V., The possible effects of the aggregation of the molecules of hemoglobin on its dissociation curves, *J. Physiol. (London)* **40**: 4–7, 1910.
- Holford N. H. G. and Sheiner L. B., Understanding the dose-effect relationship: clinical application of pharmacokinetic-pharmacodynamic models, *Clin. Pharmacokinet.* **6**: 429–453, 1981.
- Holford N. H. G. and Sheiner L. B., Kinetics of pharmacological response, *Pharmacol. Ther.* **16**: 143–166, 1982.

- Levy G., Variability in animal and human pharmacodynamic studies, in M. Rowland *et al.* (eds.), *Variability in Drug Therapy: Description, Estimation, and Control*, Raven Press, New York, 1985, pp. 125–138, 1985.
- Oosterhuis B. and van Boxtel C. J., Kinetics of drug effects in man, *Ther. Drug Monitor.* **10**: 121–132, 1988.
- Paalzow L. K. *et al.*, Variability in bioavailability: concentration versus effect, in M. Rowland *et al.* (eds.), *Variability in Drug Therapy: Description, Estimation, and Control*, Raven Press, New York, 1985, pp. 167–185, 1985.
- Ritschel W. A. and Hussain A., Review on correlation between pharmacological response and drug disposition, *Exp. Clin. Pharmacol.* **6**: 627–640, 1984.
- Schwinghammer T. L. and Kroboth P. D., Basic concepts in pharmacodynamic modeling, *J. Clin. Pharmacol.* **28**: 388–394, 1988.

12

Predicting Pharmacokinetics in Humans

Prediction of pharmacokinetic profiles of new chemical entities in humans based on *in vitro* or *in vivo* preclinical data is an extremely useful tool for drug discovery and development to identify compounds with desirable pharmacokinetic properties. There are basically two different approaches for the prediction of the pharmacokinetics of compounds in humans: allometry and the physiologically based method.

12.1. ALLOMETRY

In vivo pharmacokinetic data from experiments with various laboratory animals can be used to predict pharmacokinetic profiles in humans with allometry. Allometric extrapolation of pharmacokinetics among different species is based on the underlying anatomical, physiological, and biochemical similarities among animals (Boxenbaum, 1982; Boxenbaum and D'Souza, 1990; Dedrick, 1973).

12.1.1. Definition

Allometry, literally “by a different measure,” is the study of empirical relationships between observations such as physiological functions or the pharmacokinetics of a drug on the one hand, and the size, shape, body surface area, and/or life span of animals on the other, without necessarily examining the underlying mechanisms. It has been found that physiological functions, e.g., energy and oxygen consumption, metabolism, cardiac output, and heart rate, are quantitatively related to an animal's body weight and/or size. It is, therefore, assumed that the pharmacokinetic parameters of a drug, such as clearance, volume of distribution, and half-life, that are governed by physiological functions, e.g., organ blood flow, glomerular filtration, volume of blood, and tissue mass, can be related to body weight and/or size as well.

12.1.2. Applications of Allometry for Predicting Pharmacokinetics in Humans

The major premise behind interspecies allometric scaling is that there is a positive correlation between the physiological functions affecting drug disposition

and the body weight of animals. For instance, the hepatic blood flow rate and the weight of the liver in different species can be expressed as $55.4 \cdot BW^{0.89}$ ml/min ($r = 0.993$) and $37.0 \cdot BW^{0.85}$ kg ($r = 0.997$), respectively, where BW is the body weight (kg) of the animal of interest (Boxenbaum and D'Souza, 1990). In fact, the hepatic blood flow rate in all species is about 1.5 ml/min/g liver weight. For a drug highly extracted by the liver, clearance will be primarily governed by the hepatic blood flow rate and it can thus be readily described allometrically. Another example is creatinine clearance, which reflects the capacity of the glomerular filtration rate. Renal clearances of a drug via glomerular filtration among different species can be expressed by an allometric equation with body weight.

The allometric approach can be useful, preferably when the following conditions are met in all the included species: (1) linear kinetics of drug disposition; (2) low or similar extent of protein binding; (3) drug elimination predominantly via physical or mechanical processes (e.g., hepatic blood flow or glomerular filtration); and (4) a sufficient number of animal species and enough experimental data for linear regressions of allometric equations. There are, however, plenty of examples in which these criteria are not met, yet a reasonable prediction of pharmacokinetics in humans can be made, and vice versa.

12.1.2.1. Allometric Equations

The most commonly used allometric equation for interspecies extrapolation of pharmacokinetic parameters is (Mordenti, 1986):

(12.1)

$$Y = \alpha \cdot X^\beta$$

where Y is the pharmacokinetic parameter of interest, such as clearance and volume of distribution, and X is the physiological parameter, usually body weight. The estimates of the allometric coefficient (α) and the allometric exponent (β) can be obtained, respectively, from an intercept and a slope of a log–log plot of Eq. (12.1) (Fig.12.1).

(12.2)

$$\log Y = \log \alpha + \beta \cdot \log X$$

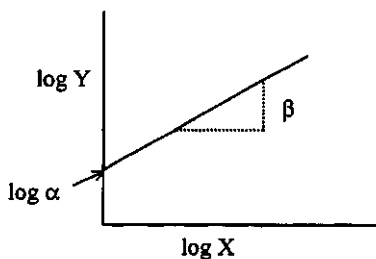


Figure 12.1. Allometric equation on a log–log scale.

Table 12. 1. Experimentally Determined Systemic Plasma Clearance (Cl_s) and Volume of Distribution (V_{ss}) of a Hypothetical Drug in Rats, Monkeys, and Dogs and Predicted Values for Those Parameters in Humans Based on Allometry

	Experimentally determined values in			Predicted values in humans by allometry
	Rat	Monkey	Dog	
Body weight (kg)	0.25	5	10	70
Cl _s (ml/min)	10.4	95.3	175.7	737
V _{ss} (liters)	0.5	11.7	18	140

For instance, if a compound of interest shows a systemic clearance (Cl_s) and a volume of distribution at steady state (V_{ss}) in rats, monkeys, and dogs as summarized in Table 12.1, allometric equations for human predictions are 30·BW^{0.75} and 2·BW¹, for Cl_s and V_{ss}, respectively based on Eq. (12.2) (Fig. 12.2).

Table 12.2 summarizes some of the known allometric relationships between physiological parameters and body weight among mammals (Boxenbaum and D’Souza, 1990; Mordenti, 1985, 1986).

12.1.2.2. Allometric Scaling of Clearance

(a) *Hepatic Clearance.* For drugs with high hepatic extraction, a reasonable allometric extrapolation of clearance between different species can be made. It is, however, difficult to apply allometry for drugs with intermediate to low hepatic clearance because clearance of those drugs is governed not only by hepatic blood flow rate, but also by other physiological and biological factors, including the

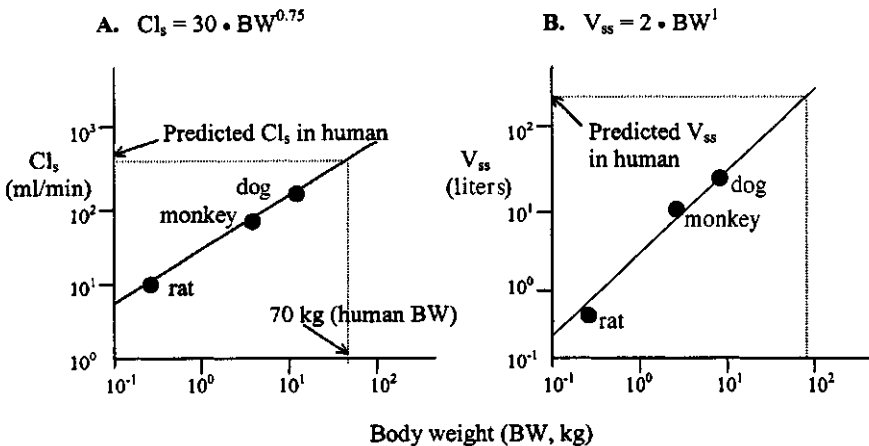


Figure 12.2. Allometric scaling for systemic clearance (Cl_s) and volume of distribution at steady state (V_{ss}) of a drug in humans. Allometric equations and plots for Cl_s (A) and V_{ss} (B) on a log–logscale are based on the animal data summarized in Table 12.2.

Table 12.2. Allometric Relationship, $Y = \alpha \cdot X^\beta$, between Physiological Parameters (Y) and Body Weight (X, kg) among Mammals

Physiological parameters	α	β	r^b
Cardiac output (ml/min)	166	0.79	—
Hepatic blood flow rate (ml/min)	55.4	0.89	0.993
Renal blood flow rate (ml/min)	43.06	0.77	—
Time for circulation of blood volume (min)	0.35	0.21	0.98
Cytochrome P450 weight (mg)	33.1	0.84	—
Nephra number	1.88×10^5	0.62	—

^aData taken from Boxenbaum and D'Souza (1990) and Mordenti (1985, 1986).

^b r is the correlation coefficient.

activities of metabolizing enzymes, to which it is difficult to apply allometry. For drugs eliminated mainly by the hepatic cytochrome P450 enzymes and classified as low-clearance drugs, the clearance predicted in humans with allometry tends to be higher than the measured value. In this case, physiologically based methods may be more appropriate.

(b) *Renal Clearance.* A relatively reasonable interspecies extrapolation can be done for renal clearance with allometry if the extent of protein binding is similar among the different species. This is because renal elimination of a drug is essentially via either physical filtration (glomerular filtration) or passive processes, with the exception of active tubular secretion. The passive processes are determined in part by the physicochemical properties of the drug and its protein binding (Ritschel *et al.*, 1992).

12.1.2.3. Allometric Scaling of the Volume of Distribution

A reasonable prediction of the volume of distribution at steady state in humans can be made with allometric extrapolation if the extent of protein binding in the plasma is similar. This is because the volume of blood and the tissue mass are allometrically related to the size of the animals, and the extent of protein binding in tissues appears to be similar among different species (Mahamood and Balian, 1996a).

12.1.2.4. Allometric Prediction of Terminal Half-Life

In general, the terminal half-life ($t_{1/2}$) of a drug with plasma exposure showing a monophasic decline on a semilog scale tends to be proportional to body weight [Eq. (12.3)], based on allometric equations for Cl_s , and V_{ss} (Ings, 1990):

$$Cl_s = \alpha_1 \cdot BW^{0.75}, \quad V_{ss} = \alpha_2 \cdot BW^1$$

(ml/min) (kg) (liters) (kg)

and thus

$$(12.3) \quad t_{1/2} \propto BW^{0.25}$$

12.1.2.5. Neoteny

There are a number of examples where simple allometry based on body weight is not adequate for prediction of systemic clearance. This apparent deviation of allometric extrapolation can be improved by introducing the concepts of neoteny into the allometric equations. Neoteny means the retention of formerly juvenile characters by adult descendants produced by retardation of somatic development, i.e., a sort of sustained juvenilization or slow development of animals to adulthood. Related it to humans, neoteny is the preservation in adults of shapes and growth rates that characterize juvenile stages of ancestral primates (Boxenbaum and D'Souza, 1990). For instance, humans tend to reach puberty at about 60% of their final body weight, whereas most other mammals reach puberty at about 30% of their ultimate body weight. The concept of maximum life span (MLP), which appears to be an allometric function of brain and body weights, has been introduced to correct for such an evolutionary development in allometric scaling:

$$(12.4) \quad \text{MLP (years)} = (185.4) \cdot \text{Br}^{0.636} \cdot \text{BW}^{-0.225}$$

The scale of both brain weight (Br) and body weight (BW) is kg (Mahamood and Balian, 1996*b*; Sacher, 1959). For instance, the MLP in humans based on 70 kg BW is approximately 88.3 years. So, e.g., the allometric relationship between Cl_s and BW can be adjusted by MLP as follows:

$$(12.5) \quad \text{Cl}_s = \frac{\alpha \cdot \text{BW}^\beta}{\text{MLP}}$$

Sometimes, the allometric relationship for low-clearance drugs can be better established with Br, rather than with MLP and BW (Ings, 1990):

$$(12.6) \quad \text{Cl}_s = \alpha \cdot \text{Br}^{\beta_1} \cdot \text{BW}^{\beta_2}$$

12.2. PHYSIOLOGICALLY BASED APPROACH

Another method for pharmacokinetic prediction in humans is based on actual physiological, anatomical, and biochemical factors important in drug disposition such as:

1. Organ blood flow rates.
2. Organ size.
3. Tissue and fluid volumes.
4. Blood-to-plasma and tissue-to-plasma drug concentration ratios.
5. Protein binding.
6. Metabolizing enzyme activities, etc.

This method offers a mechanistic approach to the extrapolation of *in vitro* experimental findings to *in vivo* pharmacokinetic parameters within the same species.

12.2.1. Predicting Systemic Clearance of a Drug in Humans from *In Vitro* Data

When metabolism is the major elimination pathway of a drug in animals and is expected to be so in humans as well, simple allometric scaling may not be adequate for prediction of clearance in the latter owing to a substantial interspecies variability in metabolism (Calabrese, 1986). In recent years, substantial progress has been made in *in vitro* metabolism studies of xenobiotics, using, e.g., purified enzymes, subcellular fractions (liver microsomes and S9), whole cells (primary hepatocytes), and liver slices (Miners *et al.*, 1994). With the sensitivity and quantitative capability of modern analytical chemistry, the utility of these *in vitro* methodologies to predict *in vivo* hepatic clearance in humans becomes of great interest (Iwatsubo *et al.*, 1997).

The well-stirred and parallel-tube models are the two most commonly used clearance models for describing *in vivo* hepatic clearance (Cl_h) of drugs.

WELL-STIRRED MODEL:

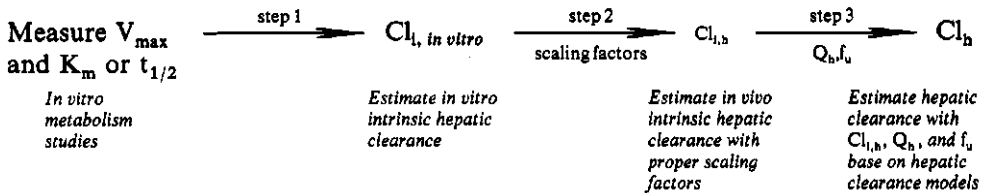
$$(12.7) \quad Cl_h = \frac{Q_h \cdot f_u \cdot Cl_{i,h}}{Q_h + f_u \cdot Cl_{i,h}}$$

PARALLEL-TUBE MODEL:

$$(12.8) \quad Cl_h = Q_h \cdot (1 - e^{-f_u \cdot Cl_{i,h}/Q_h})$$

where Q_h , f_u , and $Cl_{i,h}$ are hepatic blood flow rate, the ratio of the unbound to total drug concentrations in blood, and the intrinsic hepatic clearance, respectively. As indicated in these equations, Cl_h of a drug is affected by these three factors. It is thus possible to calculate Cl_h if those parameters are estimated or measured experimentally *in situ* or *in vitro*. In general, Q_h values reported in literature can be used. The value for f_u can be experimentally determined. The key information needed to estimate Cl_h is $Cl_{i,h}$ for the metabolic activities in the liver. It has been demonstrated that $Cl_{i,h}$ estimated from various *in vitro* metabolism studies can be used for *in vivo* Cl_h prediction with a high degree of success, if the major elimination pathway of a drug is via hepatic metabolism (Houston 1994; Houston and Carlie, 1997).

A three-step strategy to extrapolate *in vitro* metabolism data of a drug to *in vivo* hepatic clearance in animals is as follows.



Step 1: Estimate the *in vitro* intrinsic hepatic clearance $Cl_{i, in vitro}$ based on V_{max} (the maximum rate of metabolism) and K_m (the Michaelis–Menten constant for the drug–enzyme interaction), or half-life of drug disappearance ($t_{1/2}$) in *in vitro* metabolism studies.

Step 2: Extrapolate $Cl_{i, in vitro}$ to *in vivo* intrinsic hepatic clearance ($Cl_{i,h}$) with proper scaling factors.

Step 3: Calculate *in vivo* Cl_h , according to hepatic clearance models with estimates of $Cl_{i,h}$, Q_h , and f_u .

Extrapolation processes from *in vitro* metabolism data to *in vivo* hepatic clearance will be discussed based mainly on metabolic stability studies in liver microsomes and hepatocytes; however, the same approaches can be applied to other *in vitro* systems, such as liver S9 or slices. In order for extrapolation to be successful, an *in vitro* study should be performed under linear conditions in terms of incubation time, and enzyme and substrate concentrations. A detailed description of each step is given below.

12.2.1.1. Estimation of In Vitro Intrinsic Hepatic Clearance ($Cl_{i, \text{in vitro}}$)

The true *in vivo* intrinsic hepatic clearance combines the activities of the metabolizing enzymes and hepatobiliary excretion. There are, however, no reliable methods for extrapolating *in vitro* or *in situ* data to *in vivo* biliary excretion in humans. Thus, intrinsic drug clearance measured in liver microsomes or hepatocytes that only represent metabolic activities in the liver [referred to, hereafter, as *in vitro* intrinsic hepatic clearance ($Cl_{i, \text{in vitro}}$)] will be considered for *in vivo* extrapolation, so estimates of Cl_h based on $Cl_{i, \text{in vitro}}$ that do not incorporate biliary excretion may be too low.

The utility of these *in vitro* experiments for predicting clearance is based on the assumption that there is a correlation between the rate of drug disappearance (or the rate of metabolite formation) and the *in vivo* metabolic clearance of the drug. Rate data generated from certain *in vitro* systems may underestimate the true metabolic clearance *in vivo* owing to limitations in discerning metabolic capability. For instance, isolated microsomes, which are a subcellular fraction, contain only a portion of the total range of drug-metabolizing enzymes present in the original tissue *in vivo*, and thus microsomal incubations may underestimate the true metabolic clearance if the compound undergoes metabolism via cytosolic or mitochondrial enzymes *in vivo*. Nevertheless, recent studies have demonstrated that a successful quantitative extrapolation of *in vitro* metabolism data to *in vivo* clearance could be achieved under carefully designed conditions with a few assumptions (Houston 1994; Houston and Carlie, 1997).

(a) Definition of $Cl_{i, \text{in vitro}}$. $Cl_{i, \text{in vitro}}$ can be viewed as the intrinsic ability of the hepatic metabolizing enzymes present in *in vitro* systems, such as liver microsomes, S9, hepatocytes, or liver slices, to eliminate a drug from the incubation medium (12.9). This is because the rate of drug disappearance (or metabolite formation) in *in vitro* systems depends solely on the activities of metabolizing enzymes without influences from other factors that are present *in vivo*, e.g., blood flow, drug binding to blood components, and cofactor supply. (Rane *et al.*, 1977).

$Cl_{i, \text{in vitro}} = \frac{\text{Initial rate of drug disappearance (or metabolic formation) from the incubation medium}}{\text{Unbound drug concentration available to the metabolizing enzymes}}$

(12.9)

Although the drug disappearance rate can be replaced by the rate of formation of all the metabolites of the drug, for simplicity hereafter only the drug disappearance rate will be used to describe $Cl_{i, \text{ in vitro}}$. Disappearance of a drug via the metabolizing enzymes can be viewed as an enzymatic reaction describable by Michaelis–Menten kinetics:

$$(12.10) \quad \text{Rate of drug disappearance} = \frac{V_{\max} \cdot C_{1,u}}{K_m + C_{1,u}}$$

where V_{\max} and K_m are the maximum *initial* disappearance rate of a drug and the apparent Michaelis–Menten constant of total enzymes involved in its elimination in the medium, respectively. There is usually more than one enzyme metabolizing a drug, and each has its own V_{\max} and K_m for the substrate, which contributes to the *apparent* overall V_{\max} and K_m values measured. $C_{1,u}$ is the concentration of drug not bound to microsomal proteins or macromolecules in hepatocytes, which is available to the metabolizing enzymes. From Eqs. (12.9) and (12.10) $Cl_{i, \text{ in vitro}}$ can be expressed as

$$(12.11) \quad Cl_{i, \text{ in vitro}} = \frac{(V_{\max} \cdot C_{1,u}) / (K_m + C_{1,u})}{C_{1,u}} = \frac{V_{\max}}{K_m + C_{1,u}}$$

When $C_{1,u}$ is less than 10% of K_m (linear condition), $Cl_{i, \text{ in vitro}}$ can be viewed simply as the ratio between V_{\max} and K_m [Eq. (12.12)], and becomes independent of the drug concentration (Chenery *et al.*, 1987):

$$(12.12) \quad \boxed{Cl_{i, \text{ in vitro}} = V_{\max} / K_m \text{ (under linear conditions)}}$$

NOTE: *IN VIVO* INTRINSIC HEPATIC CLEARANCE ($Cl_{i,h}$). $Cl_{i,h}$ is a measure of the intrinsic ability of all the metabolizing enzymes and biliary excretion mechanisms to eliminate a drug, which is not influenced by other physiological factors that affect $Cl_{i,h}$.

(b) *Unit of $Cl_{i, \text{ in vitro}}$.* In general,

- $\mu\text{l}/\text{min}/\text{mg}$ protein: flow rate (ml/min) normalized by protein concentration when the study is performed in liver microsomes or
- $\mu\text{l}/\text{min}/10^6$ hepatocytes: normalized by number of cells when hepatocytes are used.

(c) *Estimating $Cl_{i, \text{ in vitro}}$.* There are two different methods for estimating $Cl_{i, \text{ in vitro}}$ from *in vitro* metabolism studies with liver microsomes or hepatocytes, based on: (1) estimation of V_{\max} and K_m of the metabolizing enzymes in the systems, or (2) half-life of substrate disappearance during the initial phase at a single substrate concentration.

(i) *Estimation of $Cl_{i, \text{ in vitro}}$ based on V_{\max} and K_m of the metabolizing enzymes.* $Cl_{i, \text{ in vitro}}$ can be estimated by measuring V_{\max} and K_m of the metabolizing

enzymes responsible for the disappearance of a drug in *in vitro* systems under linear conditions, according to Eq. (12.12).

- *Definition and unit of V_{\max} .* V_{\max} is a theoretical maximum initial disappearance rate of a drug via all the metabolizing enzymes when the initial substrate concentration at the beginning of the reaction approaches infinity. The magnitude of V_{\max} , therefore, is dependent on the amount of active enzymes available for metabolism of the drug. When the drug concentration in the incubating medium is μM , the unit of V_{\max} is usually: (1) $\text{pmol}/\text{min}/\text{mg}$ protein, i.e., the amount of drug metabolized per unit time (pmol of drug/ min) normalized by microsomal protein concentration when the study is performed in liver microsomes (mg protein); or (2) $\text{pmol}/\text{min}/10^6$ hepatocytes, normalized by the number of cells in the incubation medium when hepatocytes are used (10^6 hepatocytes).

- *Definition and unit of K_m .* K_m is the *apparent* Michaelis–Menten constant for the interaction between a drug and all the enzymes responsible for its metabolism. K_m can be also viewed as the initial concentration of the substrate required to reach half of V_{\max} . The true K_m of an enzyme (or apparent K_m for multiple enzymes) is constant for the given enzyme, and is independent of the amount of enzyme present in the reaction medium. The unit of K_m is usually μM (or mM).

- *Estimating of V_{\max} and K_m .* V_{\max} and K_m can be estimated by fitting the Michaelis–Mentenequation to a plot of the initial disappearance rates of a drug vs. its concentrations, or by fitting the equations transformed from the Michaelis–Menten equation, such as the Lineweaver–Burk plot, to the data.

Michaelis–Menten kinetics: V_{\max} and K_m can be estimated by fitting the Michaelis–Mentenequation to the initial disappearance rates of the substrate at different drug concentrations [Eq. (12.13) and Fig. 12.3].

$$(12.13) \quad V = \frac{V_{\max} \cdot C}{K_m + C}$$

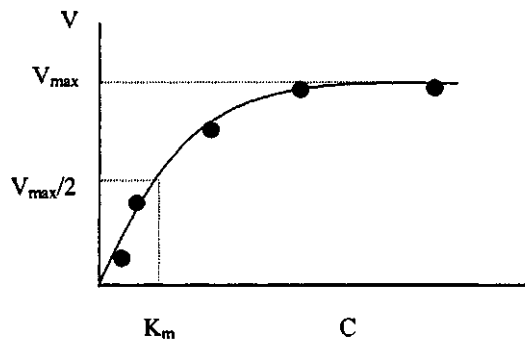


Figure 12.3. Michaelis–Menten plot (sometimes called a “substrate saturation curve”) illustrating the changes in initial disappearance rates (V) as a function of drug concentration (C). K_m is the same as the concentration at which V is a half of the theoretical maximum initial velocity (V_{\max}).

where V represents the *initial* disappearance rates of the drug at given drug concentrations (C) with a fixed amount of enzyme, i.e., a fixed amount of microsomal protein or hepatocytes.

Construction of Michaelis–Menten Plot: Several important experimental conditions are required for a proper estimate of V_{\max} and K_m from a Michaelis–Menten plot:

1. Concentration of the drug in the reaction medium should be substantially higher than the enzyme concentration.
2. Reaction conditions are established such that reliable measurement of the *initial rate* of disappearance of the drug at a given concentration is warranted. In general, initial reaction rates should be determined when less than 10% of the drug has been converted to primary metabolites in order to maintain linearity of the reaction rate. In this way, further biotransformation of metabolites to secondary or tertiary metabolites can be minimized.
3. Reaction rate should be determined at a minimum of at least five different drug concentrations (at least two and three concentrations below and above K_m , respectively).
4. For reliable estimates of V_{\max} and K_m , in general, determinations should be conducted over drug concentrations ranging from 0.1- to 10-fold of K_m .

When *initial* disappearance rates of a drug are measured, it is important to ensure that drug loss from the incubating medium equates solely with the metabolism rather than with the adsorption of the drug to apparatus or cellular components. Three important factors in determining the incubation conditions for reliable measurement of initial rates of the metabolism of a drug in *in vitro* experiments are: (a) the range of drug concentrations, (b) microsomal protein concentration (or number of hepatocytes), and (c) assay sensitivity for the drug (or its metabolites). In order to construct a Michaelis–Menten plot, several preliminary experiments have to be performed to determine optimum ranges for the drug concentration and the amount of protein.

Determination of substrate and enzymatic protein concentrations: The lowest and highest drug concentrations have to be determined during the preliminary studies for the Michaelis–Menten plot. The former can be selected based on assay sensitivity for the drug and should be substantially lower than K_m of the enzyme(s). The latter can be chosen based on the aqueous solubility of the drug. A small amount of organic cosolvent may be used to enhance solubility of lipophilic drugs, but in this case, the effects of the cosolvent on enzyme activities should be monitored and minimized (see Chapter 8).

It is also important to select a protein concentration of microsomes (or a number of hepatocytes) that yields a reliable estimate of initial drug disappearance rates. Let us assume that the disappearance profiles of a hypothetical drug at the highest concentration, 0.5 μM , are examined after incubation at three different protein concentrations of liver microsomes (Fig. 12.4). At the lowest protein concentration, the rate of drug disappearance (differences in substrate concentration

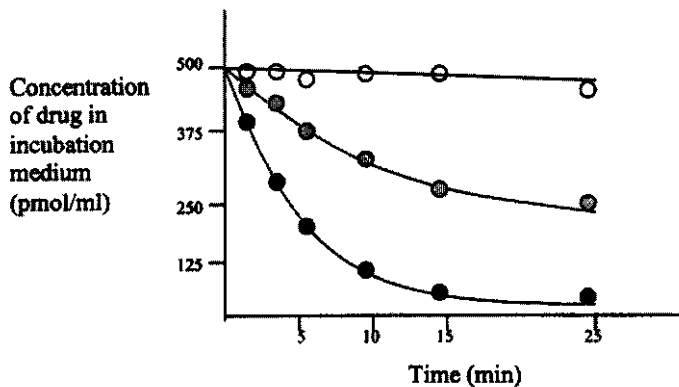


Figure 12.4. Hypothetical plot showing the changes in concentration over time after incubation of a drug at $0.5 \mu\text{M}$ in 1 ml of microsomes at three different protein concentrations (O low, \bullet medium, \circ high). The slope of the curve represents the drug disappearance rate.

over an incubation period) is consistent up to 25 min of incubation. However, consumption of the drug is less than 15% of its initial concentration, which may be difficult to distinguish reliably from the normal assay variability (usually 10–15%). At a medium protein concentration, the initial drug disappearance rate is maintained up to 10 min with approximately a 30% decrease in drug concentration. At the highest protein concentration, the drug disappearance rate is no longer the same as the initial rate shortly after incubation, which requires highly accurate time measurements and instantaneous complete mixing of drug, cofactor, and microsomes at the beginning of the experiment. From these preliminary experiments, it appears that the medium microsomal protein concentration would be the most suitable for measuring initial drug disappearance rates at $0.5 \mu\text{M}$.

Reasons for measuring initial rates: The initial rate of drug disappearance in *in vitro* metabolism should be measured for the Michaelis–Menten plot for the following reasons:

1. The concentration of a drug after incubation is lower than at the beginning of the incubation. As it is drug disappearance rates measured after incubation that are used to construct the Michaelis–Menten plot against drug concentrations at the beginning of the incubation, it is important to minimize any discrepancy caused by the difference in drug concentrations at the start and at the time of measurement.
2. Any prolonged incubation in a closed *in vitro* system such as isolated liver microsomes can cause formation of metabolites from the primary metabolites of a drug, which does not occur *in vivo*, owing to the lack of phase II metabolism and other elimination pathways.
3. Inactivation or denaturation of enzymes can become significant over time in *in vitro* systems. Thus, it is desirable to determine the initial rates during the early time points, when a significant decrease in enzyme activity is expected over time.

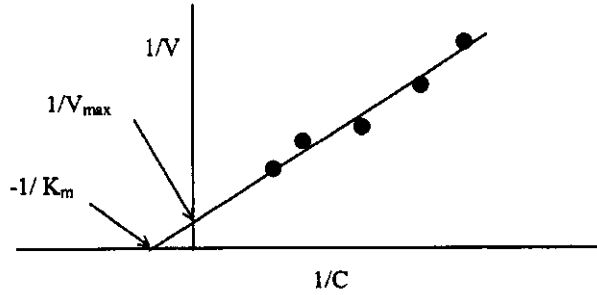


Figure 12.5. Lineweaver–Burk plot. V and C are the initial drug disappearance rate and drug concentration, respectively. The x- and y-axis intercepts of the Lineweaver–Burk plot are $-1/K_m$ and $1/V_{\max}$, respectively.

Formation rate of metabolites: When the initial formation rates of metabolites are used, the sum of the V_{\max}/K_m terms for each metabolic pathway can be used to estimate overall $Cl_{i, \text{in vitro}}$ of a drug:

$$(12.14) \quad Cl_{i, \text{in vitro}} = \frac{V_{\max,1}}{K_{m,1}} + \frac{V_{\max,2}}{K_{m,2}} + \frac{V_{\max,3}}{K_{m,3}} + \dots$$

where $V_{\max,1,2,3\dots}$ and $K_{m,1,2,3\dots}$ are maximum formation rates of each metabolite and Michaelis–Menten constants of the enzymes for the corresponding metabolites, respectively.

Lineweaver–Burk plot: It is often difficult to properly define Michaelis–Menten kinetics at high or low drug concentrations owing to limited aqueous solubility and assay limitation of a drug. The Lineweaver–Burk plot consists of reciprocals of V and C , and transforms the hyperbola of the Michaelis–Menten plot into a straight line (Fig. 12.5). It can be used to estimate V_{\max} and K_m based on data at low drug concentrations.

NOTE: RELATIONSHIPS BETWEEN MICHAELIS–MENTEN AND LINEWEAVER–BURK EQUATIONS. The Lineweaver–Burke equation is inversely related to the Michaelis–Menten equation:

MICHAELIS–MENTEN EQUATION

$$V = \frac{V_{\max} \cdot C}{K_m + C}$$

LINEWEAVER–BURK EQUATION

$$(12.16) \quad \frac{1}{V} = \frac{K_m}{V_{\max}} \cdot \frac{1}{C} + \frac{1}{V_{\max}}$$

Kinetics for multiple enzymes: When more than one enzyme is involved in the metabolism of a drug, the Lineweaver–Burk plot may become curvilinear, whereas it is less noticeable in the Michaelis–Menten plot. Thus, a Lineweaver–Burk plot (or Eadie–Hofstee plot [V vs. V/C]) is considered to be more reliable for assessing the involvement of multiple enzymes. Once those plots indicate a multienzyme system, suitable equations, shown below, can be fitted to the Michaelis–Menten plot.

MICHAELIS-MENTEN KINETICS FOR ONE ENZYME AND LINEAR KINETICS FOR THE OTHER:

$$(12.17) \quad V = \frac{V_{\max,1} \cdot C}{K_{m,1} + C} + Cl_{i,2} \cdot C$$

TWO SETS OF MICHAELIS–MENTEN EQUATIONS FOR TWO DIFFERENT ENZYMES:

$$(12.18) \quad V = \frac{V_{\max,1} \cdot C}{K_{m,1} + C} + \frac{V_{\max,2} \cdot C}{K_{m,2} + C}$$

*How to Determine V_{\max} , and K_m Experimentally and Estimate Cl_i *in vitro*:*

1. Measure the disappearance rates (V) of the drug over a linear range of the disappearance curve at more than five drug concentrations in liver microsomes (or hepatocytes). For instance, if a drug concentration decreases from 1 to 0.9 μM after 5-min in a 0.5 ml incubation buffer at a microsomal protein concentration of 1 mg/ml, an initial drug disappearance rate at 1 μM of the drug is 20 pmol/min/mg protein:

$$V = \frac{\text{Drug concentrations } (\mu\text{M}) \text{ at the beginning and after incubation}}{\text{Microsomal protein concentration in incubation buffer (mg protein/ml)}} \times \frac{1}{\text{Incubation period (min)}} = 20 \text{ (pmol/min/mg protein)}$$

Converting factor from μM to pmol/ml

The initial rate of drug disappearance (V) is usually expressed as pmol/min/mg microsomal protein or number of hepatocytes ($\times 10^6$).

2. Fit the Michaelis–Menten equation to the drug disappearance rate vs. concentration profile (the Michaelis–Menten plot) determined at five different substrate concentrations with a nonlinear regression program (e.g., PCNONLIN) for estimating of V_{\max} and K_m .

3. Calculate $Cl_{i, \text{ in vitro}}$ by dividing V_{max} by K_m [Eq. (12.12)]. For instance, if V_{max} and K_m are 100 pmol/min/mg protein and 5 μM , respectively, $Cl_{i, \text{ in vitro}}$ is 0.02 ml/min/mg protein:

$$\begin{array}{c}
 V_{\text{max}} \text{ (pmol/min/mg protein)} \\
 \downarrow \\
 Cl_{i, \text{ in vitro}} = \frac{100}{5 \times 1000} = 0.02 \text{ (ml/min/mg protein)} \\
 \begin{array}{cc}
 \nearrow & \nwarrow \\
 K_m \text{ (}\mu\text{M)} & \text{Converting factor from } \mu\text{M to pmol/ml}
 \end{array}
 \end{array}$$

(ii) *Estimating $Cl_{i, \text{ in vitro}}$ based on the half-life of drug disappearance.* $Cl_{i, \text{ in vitro}}$ can be also estimated from the half-life of initial drug disappearance at a single drug concentration substantially lower than K_m of the enzyme [Eq. (12.19)]. This approach is useful, especially when it is difficult to carry out the Michaelis–Menten kinetics experiments over a wide range of concentrations (Chenery *et al.*, 1987):

(12.19)

$$Cl_{i, \text{ in vitro}} = \frac{0.693}{t_{1/2} \cdot \text{microsomal protein concentration}}$$

$t_{1/2}$ is the half-life of drug disappearance:

(12.20)

$$t_{1/2} = \frac{(0.693) \cdot (t_2 - t_1)}{\ln(C_1/C_2)}$$

C_1 and C_2 are drug concentrations at time t_1 and t_2 after incubation, respectively. Certainly, this is an easier and faster method than Michaelis–Menten kinetics for estimating $Cl_{i, \text{ in vitro}}$, as long as several assumptions can be made.

First, the drug concentration at which the half-life of drug disappearance is measured is substantially lower than K_m ($< 10\%$ of K_m) to ensure a linear condition. Since this method requires only one drug concentration, it is important to choose an appropriate concentration and the right incubation conditions for linear kinetics. A concentration that is too high is not suitable because of potential substrate inhibition and a limitation in solubility, and a concentration that is too low is also inappropriate owing to assay limitation. Second, $t_{1/2}$ of drug disappearance should be measured over a period where the disappearance rate is linear (usually $< 10\%$ of the disappearance rate of the initial concentration of the drug). In the case of low-clearance drugs, measuring $t_{1/2}$ during the period when up to 30% of the drug disappears may be acceptable. Owing to these restrictions, an estimate of $Cl_{i, \text{ in vitro}}$ based on this method tends to be lower than that from V_{max} and K_m estimated from the Michaelis–Menten plot. Nevertheless, its experimental simplicity offers an advantage over other more complicated methods, especially during drug discovery when a crude rank order of a large number of compounds in potential metabolic clearance in humans is sufficient for compound selection.

Table 12.3. Physiological and Biochemical Parameters Important for Scaling up *In Vitro* Intrinsic Hepatic Clearance to *In Vivo* Intrinsic Hepatic Clearance and for Estimating Hepatic Clearance in Humans

Physiological parameters	Values from literature	Scaling factors ^d
Liver weight	25.7 g liver/kg body weight ^b	—
Hepatic blood flow rate	20.6 ml/min/kg body weight ^b	—
Hepatocyte number	120 × 10 ⁶ cells/g liver	3100
P450 contents in hepatocytes	0.14 nmol/10 ⁶ cells	—
Microsomal protein	52.5 mg protein/g liver	1350
	77 mg protein/g liver	1980
P450 contents in microsomes	0.32 nmol/mg microsomal protein	—
	0.296 nmol/mg microsomal protein	—

^aData taken from Bäämhielm *et al.* (1986), Davies and Morris (1993), and Iwatsubo *et al.* (1997).

^bScaling factors for estimating *in vitro* intrinsic hepatic clearance normalized by kg body weight in humans (ml/min/kg body weight), when *in vitro* intrinsic hepatic clearance is expressed as ml/min/mg microsomal protein (or ml/min 10⁶ hepatocytes).

^cAssuming that an average human body weight is 70 kg.

For instance, if *t*_{1/2} of drug disappearance is 30 min over a linear range of the drug concentration–time profile at an initial concentration of 2 μM in 0.5 ml of incubation buffer at a microsomal protein concentration of 1 mg/ml, *Cl*_{i, *in vitro*} becomes 0.02 ml/min/mg protein:

$$Cl_{i, \text{in vitro}} = \frac{\text{Constant}}{t_{1/2} \times P} = \frac{0.693}{30 \times 1} = 0.02 \text{ ml/min/mg protein}$$

↑
↑

Half-life (min)
Microsomal protein concentration in incubation buffer (mg protein/ml)

12.2.1.2. Extrapolation from *Cl*_{i, *in vitro*} to *In Vivo* Intrinsic Hepatic Clearance (*Cl*_{i,h})

Extrapolation of *Cl*_{i, *in vitro*} to *Cl*_{i,h} can be achieved by scaling up the microsomal protein (or P450) concentration (or, where relevant, the number of hepatocytes) used in *in vitro* studies to that of the whole liver. Proper scaling factors in humans and rats are summarized in Tables 12.3 and 12.4, respectively. For instance, if an estimated *Cl*_{i, *in vitro*} is 0.02 ml/min/mg microsomal protein measured after incubating a drug in human liver microsomes, *Cl*_{i,h} of the drug in human liver *in vivo* can be estimated by multiplying *Cl*_{i, *in vitro*} by a scaling factor of 1350 (or 1980) (Table 12.3), i.e.,

$$Cl_{i,h} = 0.02 \times 1350 = 27 \text{ (ml/min/kg body weight)}$$

↑
↑

*Cl*_{i, *in vitro*} (ml/min/mg microsomal protein)
Scaling factor

Table 12.4. Physiological and Biochemical Parameters Important for Scaling up *In Vitro* to *In Vivo* Intrinsic Clearance and for Estimating Hepatic Clearance in Rats^a

Physiological parameters	Published values	Scaling factors ^b
Liver weight	45 g liver/kg body weight ^c	—
Hepatic blood flow rate	81 ml/min/kg body weight ^c	—
Hepatocyte number	135×10^6 cells/g liver	6100
Microsomal protein	45 mg proteins/g liver	2000
	54 mg protein/g liver	2400
P450 contents in microsomes	0.98 nmol/mg microsomal protein ^d	—

^aData taken from Bäärnhielm *et al.* (1986) and Houston (1994).

^bScaling factors for estimation of *in vivo* intrinsic hepatic clearance in rat normalized by kg body weight (ml/min/kg body weight), when *in vitro* intrinsic hepatic clearance is expressed as ml/min/mg microsomal protein (or ml/min/10⁶hepatocytes).

^cAssuming that an average body weight of rat is 0.25 kg.

^dBäärnhielm *et al.*, 1986.

where the scaling factor is 52.5 mg microsomal protein/g liver multiplied by 25.7 g liver/kg body weight in humans which is equal to 1350 mg microsomal protein/kg body weight. Thus, the unit of $Cl_{i,h}$ becomes ml/min/kg body weight.

12.2.1.3. Utilization of Hepatic Clearance Models to Estimate *In Vivo* Hepatic Clearance of a Drug

Estimates of *in vivo* hepatic clearance (Cl_h) can be achieved by incorporating estimates of $Cl_{i,h}$, Q_h , and f_u into the hepatic clearance model(s). For instance, if 90% of a drug is bound to blood components ($f_u = 0.1$) and $Cl_{i,h}$ is estimated at 27 ml/min/kg body weight, Cl_h of the drug in humans *in vivo* is then 2.66 or 2.53 ml/min/kg body weight, according to the well-stirred or parallel-tube models for hepatic clearance, respectively.

Table 12.5. Concentration of Cytochrome P450 and the Amount of Microsomal Protein per Gram of Liver in Rats, Dogs, and Humans (Mean \pm SD)

Species	Cytochrome P450 (nmol/mg protein)	Microsomal protein concentration (mg/g liver)	Liver weight (g/kg body weight)
Rat	0.980 ± 0.10^a	54 ^a , 45 ^b	42.4 ^a , 45 ^b
Dog	0.474 ± 0.080^a 0.78 ± 0.08^c	43 ^a —	25.6 ^a —
Human	0.296 ± 0.093^a , 0.32 ^d	77 ^a , 52.5 ^d	20.2 ^a

^aData taken from Bäärnhielm *et al.* (1986).

^bData taken from Houston (1994).

^cData taken from Duignan *et al.* (1987).

^dData taken from Iwatsubo *et al.* (1997).

WELL-STIRRED MODEL:

$$\begin{aligned}
 Cl_h &= \frac{Q_h \cdot f_u \cdot Cl_{i,h}}{Q_h + f_u \cdot Cl_{i,h}} = \frac{\overset{\text{ml/min/kg body weight}}{20.6} \times \overset{\text{no unit}}{0.1} \times \overset{\text{ml/min/kg body weight}}{27}}{20.6 + 0.1 \times 27} \\
 &= 2.66 \text{ ml/min/kg body weight}
 \end{aligned}$$

PARALLEL-TUBE MODEL:

$$Cl_h = Q_h \cdot (1 - e^{-f_u \cdot Cl_{i,h}/Q_h}) = 2.53 \text{ ml/min/kg body weight}$$

Differences in the estimates of Cl_h from these two models are less important for low-clearance drugs, i.e., drugs with $f_u \cdot Cl_{i,h} \ll Q_h$. When the extraction ratio of a drug is greater than 0.7, the difference in the clearance estimate between the models becomes more apparent. Despite its assumptions and simplifications, the well-stirred model, the least sophisticated of the hepatic clearance models, appears to suffice for extrapolation of *in vitro* metabolism data to *in vivo* clearance. Similarly, the simple Michaelis–Menten kinetics is considered to be adequate for describing kinetic behaviors of metabolizing enzymes, despite the known complexities of enzyme families and reaction patterns.

12.2.1.4. Comparison of Various In Vitro Methods for Predicting In Vivo Hepatic Clearance

In general, primary hepatocytes (freshly isolated hepatocytes) seem to provide more reliable *in vitro* predictions of Cl_h than liver microsomes or slices. Studies using liver microsomes or slices tend to underestimate Cl_h as compared to hepatocytes. It has been found that the rate of drug metabolism in hepatocytes is approximately three times as fast as that in microsomes when normalized by microsomal protein concentration (Houston and Carlie, 1997; Miners *et al.*, 1994). The slower metabolism rate in microsomes can be the result of various factors. For instance,

1. Limited metabolic capability of microsomes: Hepatocytes can perform both phase I and phase II metabolism, whereas microsomes have phase I metabolism or only limited phase II metabolism such as UDP-glucuronosyl transferase activity depending on reaction conditions.
2. Damage to microsomes during preparation: Structural integrity of microsomes may be damaged to a certain extent during isolation owing to the disruptive nature of the preparation processes, and subsequent reestablishment of study conditions for metabolism may not be physiologically optimal.
3. Inactivation of enzymatic activities in microsomes: When the half-life of drug disappearance is used to estimate Cl_i , *in vitro* rather than the Michaelis–Menten kinetics for separate V_{max} and K_m estimates, liver microsomes may not be able to maintain full activity over a sufficiently long incubation period for an accurate measurement of the half-life.

4. Nonspecific binding of drug to microsomal proteins: In microsomes, any nonspecific binding of a drug to microsomal proteins (usually 10 to 60% in rat liver microsomes at 1 mg microsomal protein) may cause the concentration of the drug available to the enzyme to be lower than that initially added in the reaction medium. On the other hand, the extent of nonspecific binding of a drug to intracellular protein in hepatocytes may be lower than in microsomal preparations, when normalized by enzyme activities.

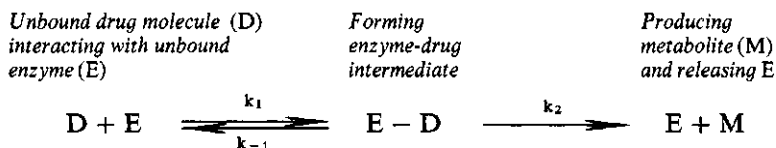
Comparison between microsomes and hepatocytes for prediction in vivo clearance: Extrapolations from studies with hepatocytes tend to be more reliable than those from microsomes. For low-clearance drugs ($Cl_{i, \text{ in vitro}} < 20 \mu\text{l}/\text{min}/\text{mg}$ microsomal protein), prediction is reasonable; however, for high-clearance drugs ($Cl_{i, \text{ in vitro}} > 100 \mu\text{l}/\text{min}/\text{mg}$ microsomal protein), predicted values of Cl_h based on microsomal data are substantially lower than those from the corresponding hepatocyte data or measured Cl_h .

Using liver slices for predicting in vivo clearance: Liver slices have not been used as extensively as microsomes or primary hepatocytes for predicting Cl_h for the following reasons:

1. Difficulties in preservation and limited availability of fresh liver slices: Only limited success in cryopreservation of slices.
2. Lack of population approach: Difficulties in phenotyping liver slices from different individuals prior to the studies.
3. Diffusion (transport)-limited metabolism: Because of the limited diffusibility of a drug across the multilayers of hepatocytes in slices (approximately five layers of hepatocytes in about 200- μm -thick slices), drug metabolism takes place mainly in the outer layers of a liver slice. In other words, drug availability to hepatocytes in liver slices is rather limited as compared to that in isolated hepatocytes.

12.1.2.5. Effects of Nonspecific Binding of a Drug on In Vitro Metabolism

Michaelis–Menten kinetics for enzyme reactions such as metabolism is based on the interaction between *unbound* drug and *unbound* enzyme molecules in the medium, forming enzyme–drug intermediates, which then break into metabolites and *unbound* enzymes:



The initial rate of drug disappearance according to Michaelis–Menten kinetics [Eq. (12.10)] is a function of the *unbound*, not the total, drug concentration actually

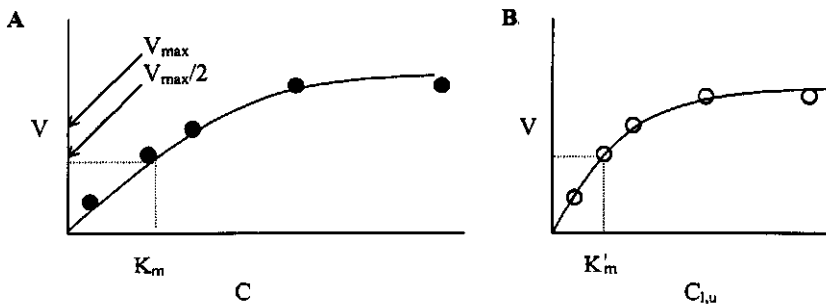


Figure 12.6. Differences in Michaelis–Menten constants obtained based on the relationship between initial disappearance rates (V) of a drug and its total (C , ●) or unbound ($C_{l,u}$, ○) concentrations in liver microsomes. K_m and K'_m are indicated as total (A) and unbound (B) drug concentrations, at which V is half of V_{max} . V_{max} is independent of nonspecific binding of the drug to microsomal proteins.

available to the metabolizing enzymes. K_m is equal to the *unbound* drug concentration in the medium at which the initial rate of drug disappearance is half of V_{max} , and thus should be determined from the relationship between the initial rate of drug disappearance and the unbound drug concentrations in the medium. V_{max} should not be affected by the extent of drug binding in the medium (Bäärnhielm *et al.*, 1986; Ito *et al.*, 1998; Obach, 1997).

For instance, when metabolism is studied in microsomes, the total concentration of the drug added to the medium may not be equal to its unbound concentration owing to the nonspecific binding to microsomal proteins. In fact, the values of K_m estimated based on total drug concentrations in the reaction medium can be significantly greater than that based on the unbound drug concentrations (Fig. 12.6). The K_m value corrected for the extent of nonspecific protein binding (K'_m) can be obtained by multiplying the value estimated based on total concentrations i.e., K_m) by the ratio of unbound and total drug concentrations in the microsomes ($f_{u,m}$):

$$(12.21) \quad \boxed{K'_m = f_{u,m} \cdot K_m}$$

$f_{u,m}$ can be estimated through protein binding studies such as equilibrium dialysis without cofactors at a single drug concentration in a reaction medium containing microsomes, if the extent of protein binding is independent of drug concentration. Nonspecific binding to microsomal proteins has been found to be 10 to 60%, i.e., $f_{u,m}$ of 0.4 to 0.9, at a microsomal protein concentration of 1 mg/ml for several drugs.

For drugs with extensive nonspecific binding, the estimate for $Cl_{i, \text{in vitro}}$ using K_m can be too low. If extensive nonspecific binding of a drug is expected, it is important to consider $f_{u,m}$ for estimating the true $Cl_{i, \text{in vitro}}$:

$$(12.22) \quad Cl_{i, \text{in vitro}} = \frac{V_{max}}{K'_m} = \frac{V_{max}}{f_{u,m} \cdot K_m}$$

Discrepancies between the predictions from in vitro data and in vivo findings: It is not uncommon to find that hepatic clearance predicted on the basis of *in vitro* data can under- or overestimate the true *in vivo* hepatic clearance (Houston and Carlie, 1997). Several potential causes for these discrepancies are as follows:

1. Underestimation of *In Vivo Hepatic Clearance*. In many cases, *in vivo* hepatic clearance (Cl_h) predicted from $Cl_{i, \text{in vitro}}$ tends to be lower than the measured Cl_h , especially for high-clearance drugs ($Cl_{i, \text{in vitro}} > 100 \mu\text{l}/\text{min}/\text{mg}$ protein). This discrepancy might be due to the following limitations of *in vitro* experiments:

- Limited metabolic activities: This becomes more apparent in liver microsome studies.
- Product inhibition by metabolites on enzyme activities: This is of concern especially in microsome studies owing to the lack of active phase II conjugating enzymes.
- Variability of *in vitro* systems (sample collection, storage condition, etc): The disruptive nature of the microsomal preparation can result in the loss of activities or variability in activities of different isoforms. In most cases, approximately 20% of the primary hepatocytes isolated using current methods are not viable.
- Poor penetration of drug into multilayers of hepatocytes in liver slices: Owing to poor penetration of the drug, drug metabolism takes place mainly in hepatocytes in the outer layer of liver slices.
- Nonspecific binding of a drug to microsomal proteins and/or experimental apparatus: Since only unbound drug is subject to metabolism, nonspecific binding of a drug in *in vitro* experiments can reduce the amount of drug available for metabolism, resulting in apparently lower $Cl_{i, \text{in vitro}}$ compared to $Cl_{i,h}$ when normalized by protein concentration.
- Inability to predict biliary clearance in *in vitro* metabolic systems.

2. Overestimation of *In Vivo Hepatic Clearance*: Occasionally, a predicted Cl_h based on $Cl_{i, \text{in vitro}}$ is higher than the measured Cl_h , which can be due to:

- A slow equilibrium of drug between sinusoidal blood and hepatocytes: When intrinsic hepatic clearance (metabolism and biliary excretion) of a drug is much faster than the efflux clearance from the hepatocytes to the sinusoidal blood, the apparent $Cl_{i,h}$ becomes governed by drug uptake from the sinusoidal blood into the hepatocytes. In this case, $Cl_{i, \text{in vitro}}$ estimated in liver microsomes, which does not account for a slow drug uptake from the blood into the hepatocytes *in vivo*, can lead to an overestimate of Cl_h (Kwon and Morris, 1997).

3. Other Factors:

- The presence of active transporters in the sinusoidal membranes of hepatocytes: When a drug is subject to active transporters located in the sinusoidal membranes, its unbound drug concentration within the hepatocytes can be different than it is in blood. The effects of active drug transport on Cl_h are often difficult to assess

Table 12.6. Known Standard Values for Volumes of Different Body Fluids in Animals and Humans

Species	Volumes (liters/kg) ^a		
	V _p	V _e	V _r
Rat, guinea pig	0.031	0.266	0.371
Rabbit	0.044	0.206	0.466
Monkey	0.045	0.163	0.485
Dog	0.052	0.225	0.328
Human	0.043	0.217	0.340

^aV_p: plasma volume; V_e: extracellular fluid volume minus plasma volume; and V_r: physical volume into which the drug distributes minus the extracellular space (intracellular fluid volume).

solely from *in vitro* data and further experiments, such as liver perfusion, are needed.

- Interindividual variability in metabolism: Genetic polymorphism and environmental factors can cause significant variability in hepatic metabolic ability and capacity among different individuals. It is, therefore, often difficult to predict Cl_h representing population from *in vitro* experiments with liver samples obtained from a few individuals.

12.2.2. Predicting the Volume of Distribution of a Drug in Humans

Equation (12.23) developed by Φie and Tozer can be used to predict the volume of drug distribution at steady state in humans using the known values for actual physiological volumes and the fractions of drug not bound to plasma components determined experimentally (Φie and Tozer, 1979). An estimate of the ratio of unbound and total drug concentrations in intracellular space (f_{ut}) of a drug in humans can be obtained by averaging f_{ut} values calculated from at least two different species [Eq. (12.24)], assuming that f_{ut} is similar across species. The known standard values for V_p, V_e, and V_r in humans are shown in Table 12.6.

$$(12.23) \quad V_{ss} = (2.4) \cdot V_p + f_u \cdot V_p \cdot [(V_e/V_p) - 1.4] + (f_u/f_{ut}) \cdot V_r$$

$$(12.24) \quad f_{ut} = \frac{f_u \cdot V_r}{V_{ss} - (2.4) \cdot V_p - f_u \cdot V_p \cdot [(V_e/V_p) - 1.4]}$$

f_u is the ratio of unbound and total drug concentrations in plasma, f_{ut} is the ratio of unbound and total drug concentrations in intracellular space (tissues), V_p is the plasma volume (liters/kg), V_e is the extracellular fluid volume minus the plasma volume (liters/kg), V_r is the physical volume into which the drug distributes minus the extracellular space (liters/kg), and V_{ss} is the volume of distribution at steady state (liters/kg).

REFERENCES

- Bäärnhielm C. *et al.*, *In vivo* pharmacokinetics of felodipine predicted from *in vitro* studies in rat, dog and man, *Acta. Pharmacol. et Toxicol.* **59**: 113–122,1986.
- Boxenbaum H., Interspecies scaling, allometry, physiological time and ground plan of pharmacokinetics, *J. Pharmacokinet. Biopharm.* **10**: 201–227,1982.
- Boxenbaum H. and D'Souza R. W., Interspecies pharmacokinetic scaling, biological design and neoteny. *Adv. Drug Res.* **19**: 139–196,1990.
- Calabrese E. J., Animal extrapolation and the challenge of human heterogeneity, *J. Pharm. Sci.* **75**: 1041–1046,1986.
- Chenery R. J. *et al.*, Antipyrine metabolism in cultured rat hepatocytes, *Biochem. Pharmacol.* **36**: 3077–3081,1987.
- Davies B. and Morris T., Physiological parameters in laboratory animals and humans. *Pharm. Res.* **10**: 1093–1095,1993.
- Dedrick R. L., Animal scale-up, *J. Pharmacokinet. Biopharm.* **1**: 435–461,1973.
- Duignan D. B. *et al.*, Purification and characterization of the dog hepatic cytochrome P450 isozyme responsible for the metabolism of 2,2',4,4',5,5'-hexachlorobiphenyl, *Arch. Biochem. Biophys.* **255**: 290–303,1987.
- Houston J. B., Utility of *in vitro* drug metabolism data in predicting *in vivo* metabolic clearance, *Biochem. Pharmacol.* **47**: 1469–1479,1994.
- Houston J. B. and Carlie D. J., Prediction of hepatic clearance from microsomes, hepatocytes, and liver slices, *Drug Metab. Rev.* **29**: 891–922,1997.
- Ings R. M. J., Interspecies scaling and comparisons in drug development and toxicokinetics, *Xenobiotica* **20**: 1201–1231,1990.
- Ito K. *et al.*, Quantitative prediction of *in vivo* drug clearance and drug interactions from *in vitro* data on metabolism, together with binding and transport, *Ann. Rev. Pharmacol. Toxicol.* **38**: 461–499,1998.
- Iwatsubo T. *et al.*, Prediction of *in vivo* drug metabolism in the human liver from *in vitro* metabolism data, *Pharmacol. Ther.* **73**: 147–171,1997.
- Kwon Y. and Morris M. E., Membrane transport in hepatic clearance of drugs. I: Extended hepatic clearance models incorporating concentration-dependent transport and elimination processes, *Pharm. Res.* **14**: 774–779,1997.
- Mahamood I. and Balian J. D., Interspecies scaling: a comparative study for the prediction of clearance and volume using two or more than two species. *Life Sci.* **59**: 579–585,1996a.
- Mahamood I. and Balian J. D., Interspecies scaling: predicting clearance of drugs in humans: three different approaches, *Xenobiotica* **26**: 887–895,1996b.
- Miners J. O. *et al.*, *In vitro* approaches for the prediction of human drug metabolism, *Ann. Rep. Med. Chem.* **29**: 307–316,1994.
- Mordenti J., Forecasting cephalosporin and monobactam antibiotic half-lives in humans from data collected in laboratory animals, *Antimicrob. Agents Chemother.* **27**: 887–891,1985.
- Mordenti J., Man versus beast: pharmacokinetic scaling in mammals, *J. Pharm. Sci.* **75**: 1028–1040,1986.
- Obach R. S., Nonspecific binding to microsomes: impact on scale-up of *in vitro* intrinsic clearance to hepatic clearance as assessed through examination of warfarin, imipramine, and propranolol, *Drug Metab. Dispos.* **25**: 1359–1369,1997.
- Qie S. and Tozer T. N., Effect of altered plasma protein binding on apparent volume of distribution, *J. Pharm. Sci.* **68**: 1203–1205,1979.
- Rane A. *et al.*, Prediction of hepatic extraction ratio from *in vitro* measurement of intrinsic clearance, *J. Pharmacol. Exp. Ther.* **200**: 420–424, 1977.
- Ritschel W. A. *et al.*, The allometric approach for interspecies scaling of pharmacokinetic parameters, *Comp. Biochem. Physiol.* **103C**: 249–253,1992.
- Sacher G. A., Relationship of life span to brain weight and body weight in mammals, in G. E. W. Wolstenholm and M. O'Connor (eds.), *CIBA Foundation Colloquium on Aging*, Churchill, London, 1959, pp. 115–133.